Electronic Supplementary Information (ESI)

Exploring Mn^{2+}-Location-Dependent Red Emission from (Mn/Zn)-Ga-Sn-S Supertetrahedral Nanocluster with Relatively Precise Dopant Position

Qian Zhang,[a] Jian Lin,[a] Yun-Tao Yang,[e] Zhen-Zhen Qin,[e] Dongsheng Li,[b] Shuao Wang,[c] Yipu Liu,[d] Xiaoxin Zou,[d] Yan-Bo Wu*[e] and Tao Wu*[a]

[a] *College of Chemistry, Chemical Engineering and Materials Science, Soochow University, Jiangsu 215123, China.*

[b] *College of Materials and Chemical Engineering, Key Laboratory of Inorganic Non-metallic Crystalline and Energy Conversion Materials, China Three Gorges University, Yichang 443002, China.*

[c] *School for Radiological and Interdisciplinary Sciences (RAD-X), Soochow University, Jiangsu 215123, China.*

[d] *State Key Laboratory of Inorganic Synthesis and Preparative Chemistry, International Joint Research Laboratory of Nano-Micro Architecture Chemistry, College of Chemistry, Jilin University, Changchun 130012, P. R. China.*

[e] *The Key Laboratory of the Materials for Energy Storage and Conversion of Shanxi Province, Institute of Molecular Science, Shanxi University, Taiyuan 030006, Shanxi, China.*

* Corresponding author: E-mail: wutao@suda.edu.cn; wyb@sxu.edu.cn

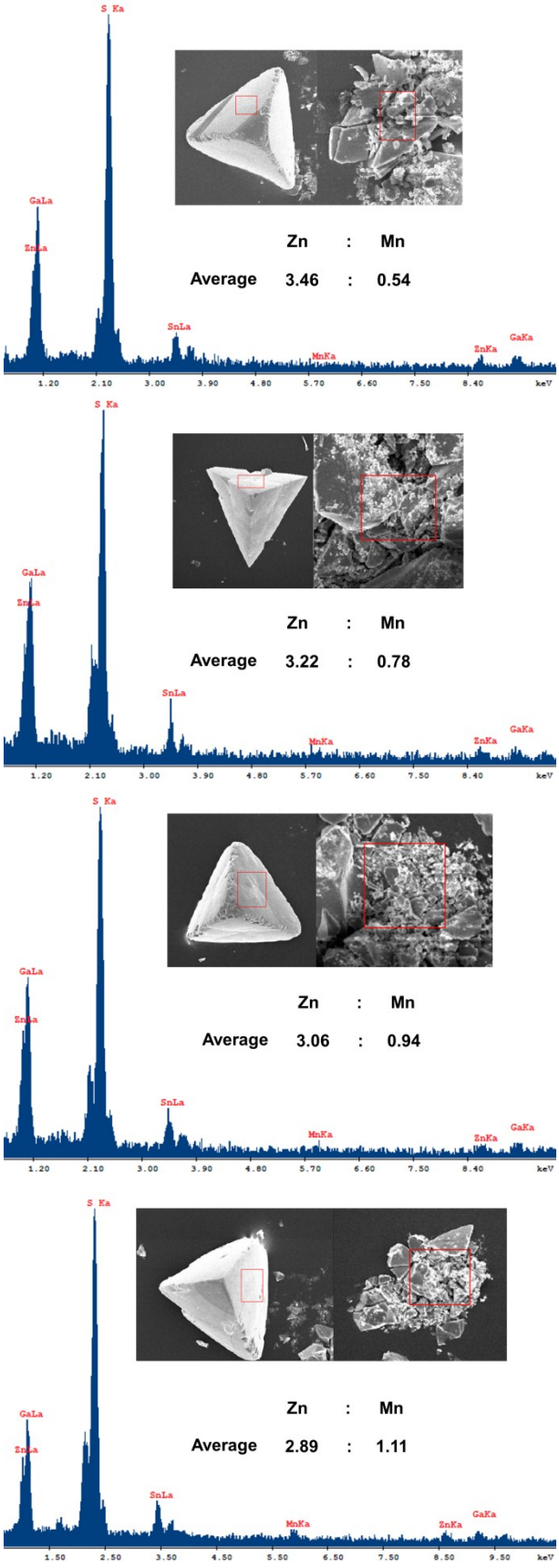

Fig. S1 EDS of four batches of Mn^{2+}-doped OCF-40-ZnGaSnS samples.

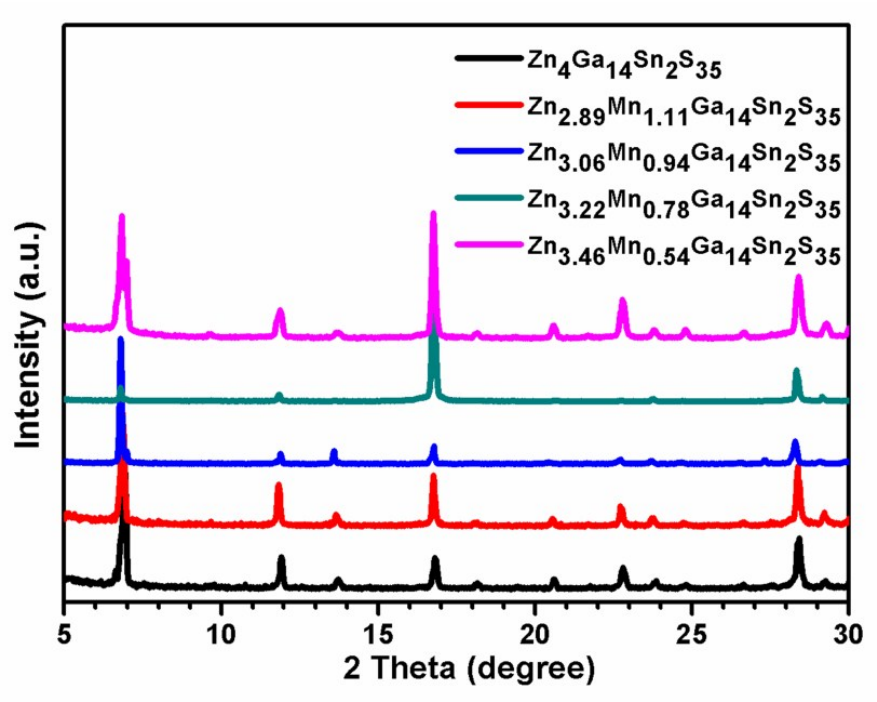

Fig. S2 PXRD patterns of Mn^{2+}-doped samples at room temperature.

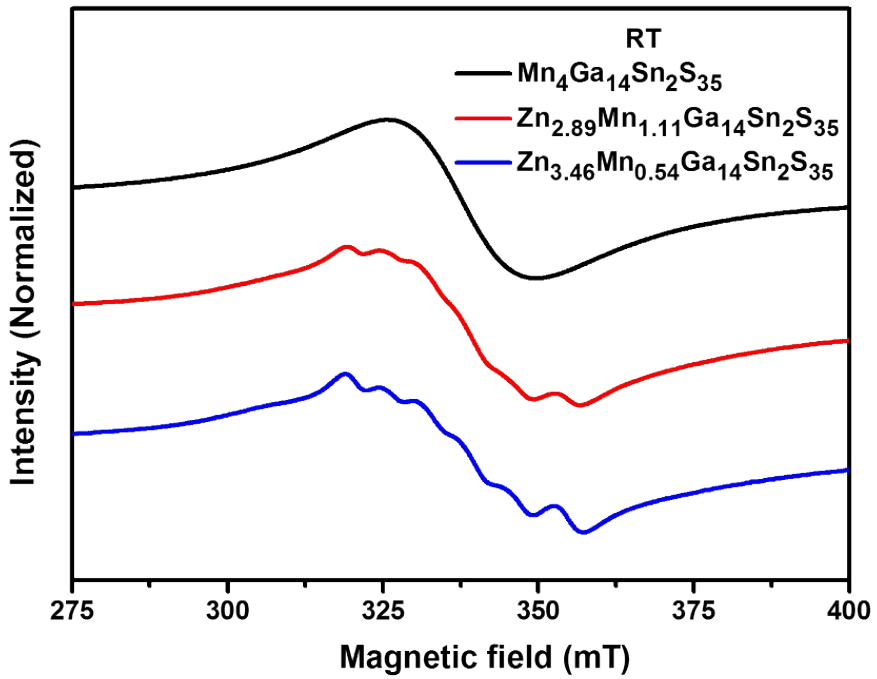

Fig. S3 EPR signals of OCF-40-MnGaSnS and Mn^{2+}-doped samples under room temperature.

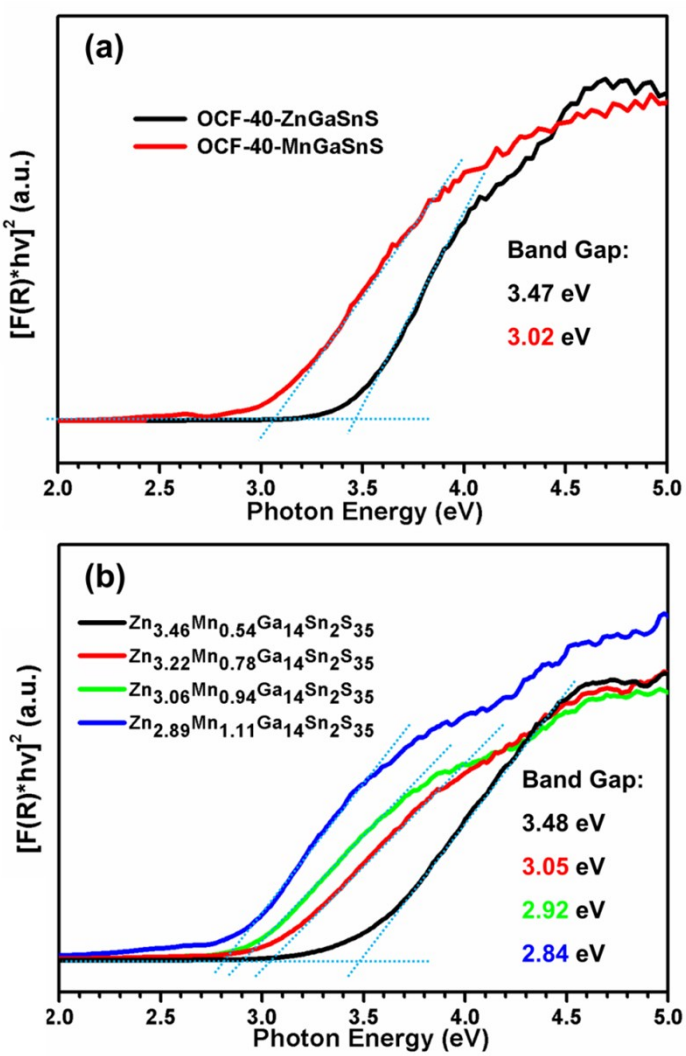

Fig. S4 Tauc plots of OCF-40-ZnGaSnS, OCF-40-MnGaSnS and Mn^{2+}-doped samples.

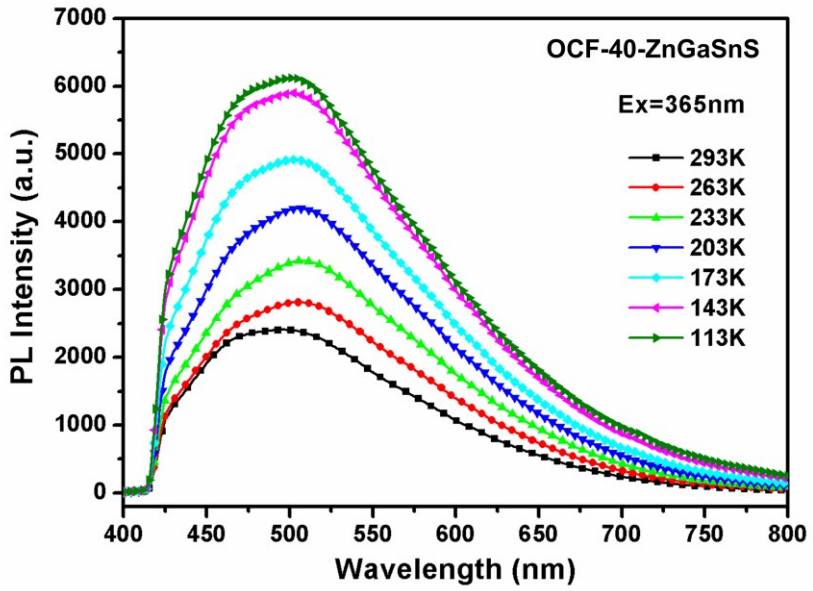

Fig. S5 Singe-crystal PL of OCF-40-ZnGaSnS excited at 365 nm.

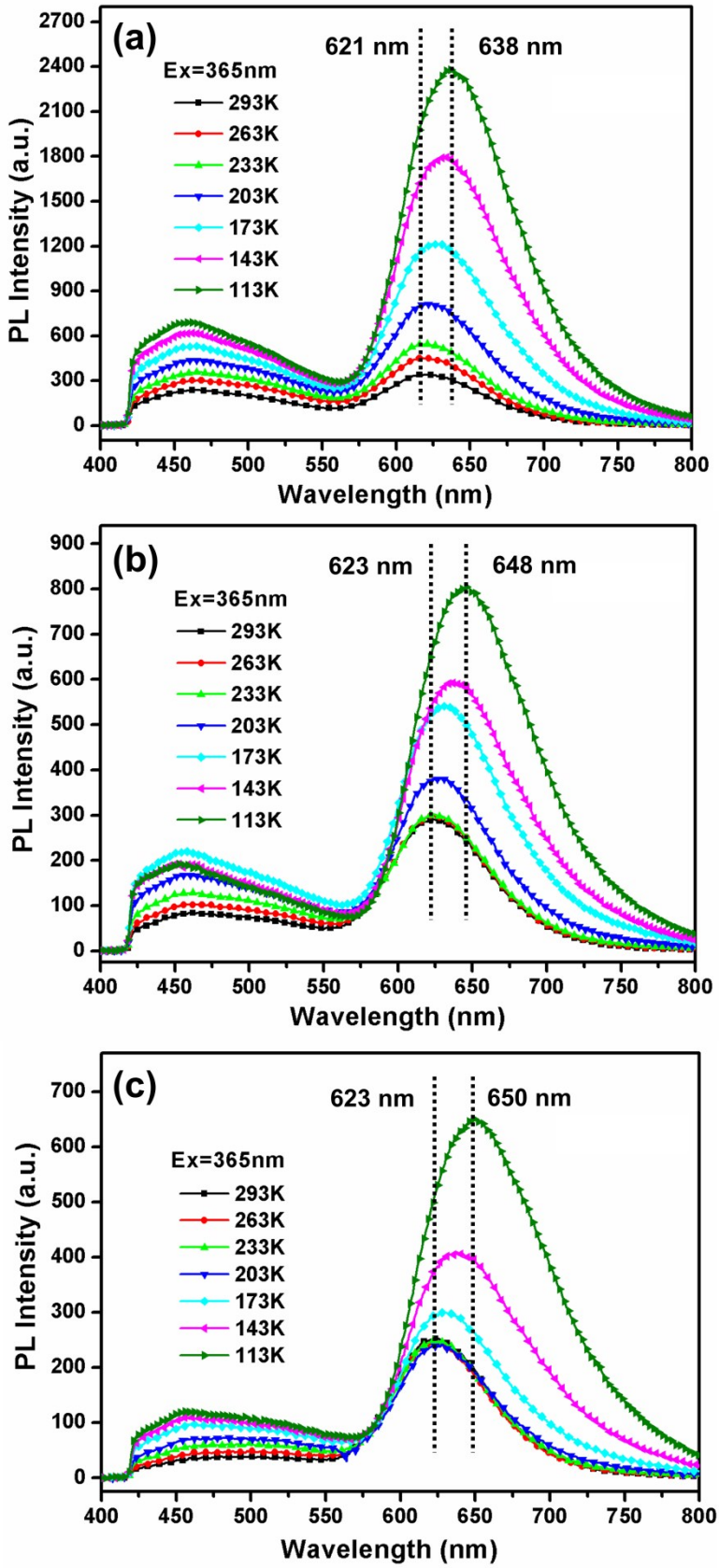

Fig. S6 Single-crystal PL spectra of Mn^{2+}-doped OCF-40-ZnGaSnS: (a) $Zn_{3.46}Mn_{0.54}Ga_{14}Sn_2S_{35}$; (b) $Zn_{3.22}Mn_{0.78}Ga_{14}Sn_2S_{35}$; (c) $Zn_{3.06}Mn_{0.94}Ga_{14}Sn_2S_{35}$.

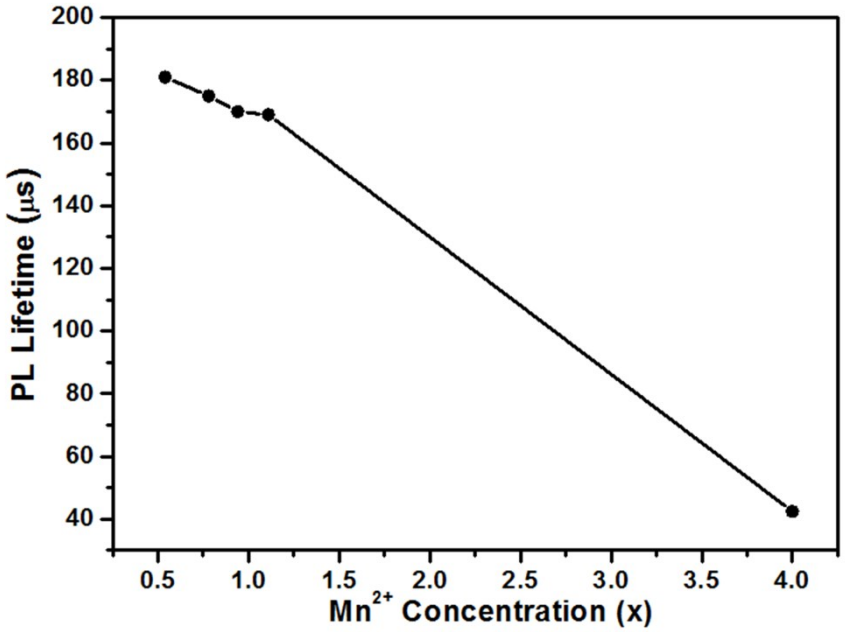

Fig. S7 Mn^{2+} concentration-dependent decay time of Mn^{2+}-doped samples monitored at 642 nm upon the excitation of 474 nm at room temperature.

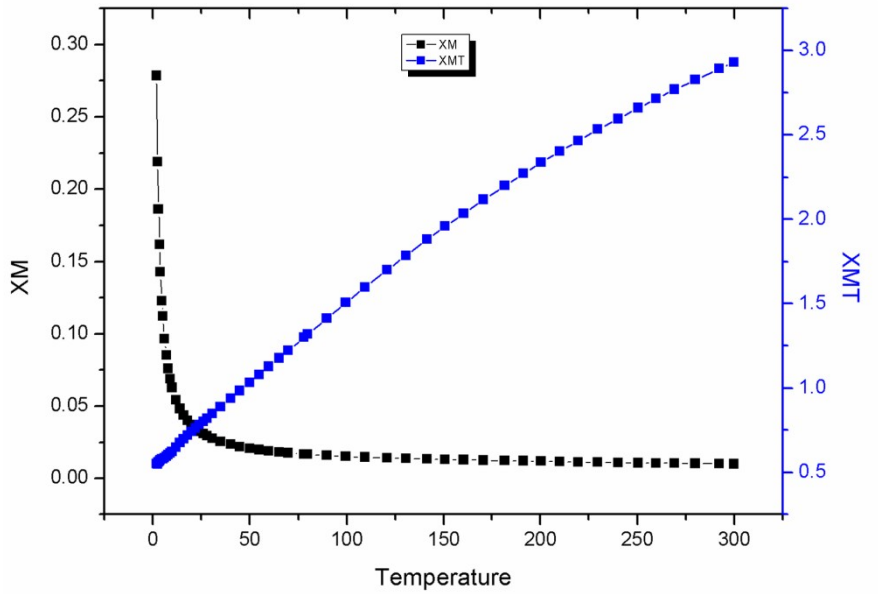

Fig. S8 The variable-temperature (2-300 K) magnetic susceptibility of the heavily-doped NC $Mn_4Ga_4Sn_2S_{35}$.

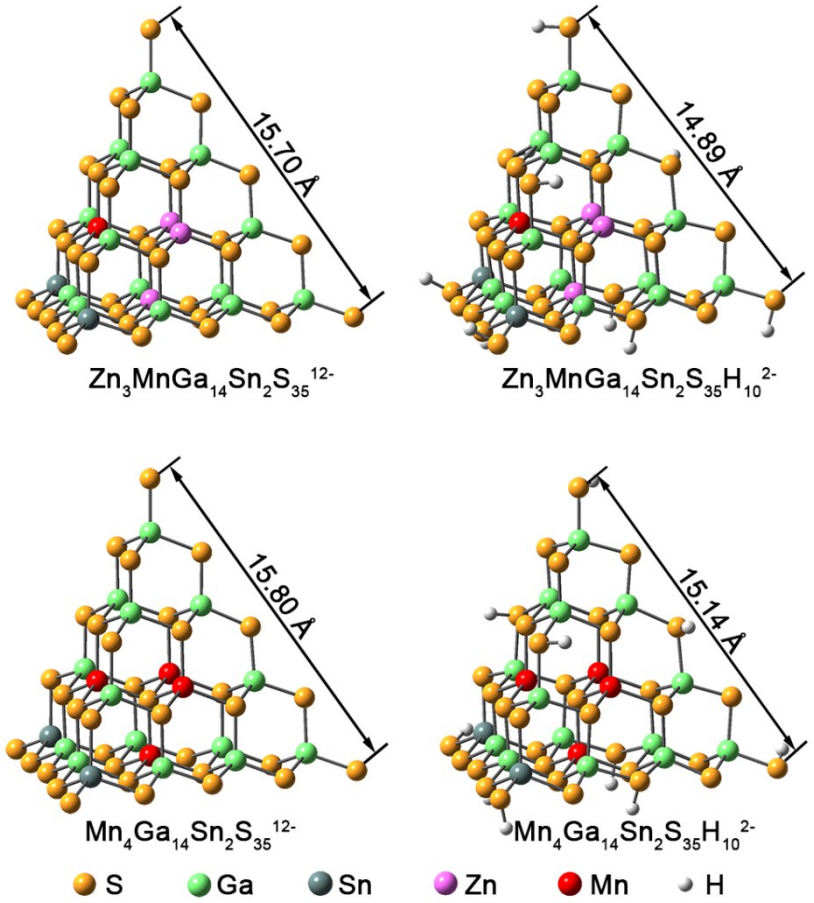

Fig. S9 Optimized structure of the bare and protonated NCs.

Table S1 The molar ratio of Zn : Mn in the Mn^{2+}-doped samples.

$Zn(NO_3)_2 \cdot 6H_2O$ (mg)	$Mn(Ac)_2 \cdot 4H_2O$ (mg)	Raw molar ratio of Zn : Mn	Actual Molar ratio of Zn : Mn	
			EDS	ICP-OES
76.9	28	2.78 : 1.22	2.89 : 1.11	3.01 : 0.99
76.9	21	3.00 : 1.00	3.06 : 0.94	2.98 : 1.02
76.9	14	3.28 : 0.72	3.22 : 0.78	/
76.9	7	3.60 : 0.40	3.46 : 0.54	/

Table S2 PL Lifetime of OCF-40-MnGaSnS monitored at the emission wavelength of 642 nm under different temperature.

Temp.	A_1 (%)	τ_1 (s)	A_2 (%)	τ_2 (s)	τ_{ave} (s)
296K	45.01	1.064058E-05	54.99	6.849213E-05	4.24528E-05
273K	35.35	9.669258E-06	64.65	7.679196E-05	5.26773E-05
243K	28.95	1.072045E-05	71.05	9.039018E-05	6.73258E-05
213K	21.01	1.235974E-05	78.99	1.122783E-04	7.39960E-05
183K	15.26	9.668174E-06	84.74	1.304276E-04	1.11999E-04
153K	12.21	1.26764E-05	87.79	1.622251E-04	1.43965E-04
123K	15.89	1.417034E-05	84.11	1.76324E-04	1.50558E-04
93K	26.75	2.898245E-05	73.25	1.95354E-04	1.50849E-04
63K	26.65	6.311241E-05	73.35	2.240722E-04	1.81176E-04

Table S3 PL Lifetime of Mn^{2+}-doped samples ($Zn_{4-x}Mn_xGa_{14}Sn_2S_{35}$) under room temperature.

χ	A_1 (%)	τ_1	A_2 (%)	τ_2	τ_{ave} (s)
4	45.01	1.064058E-05	54.99	6.849213E-05	4.24528E-05
1.11	17.39	1.79328E-05	82.61	2.003149E-04	1.68599E-04
0.94	14.87	1.644032E-05	85.13	1.969501E-04	1.70108E-04
0.78	17.12	9.2786E-06	82.88	2.089991E-04	1.74807E-04
0.54	25.34	1.188928E-05	74.66	2.378971E-04	1.80627E-04

Full form of reference 27.

M. J. Frisch, G. W. Trucks, H. B. Schlegel, G. E. Scuseria, M. A. Robb, J. R. Cheeseman, G. Scalmani, V. Barone, B. Mennucci, G. A. Petersson, H. Nakatsuji, M. Caricato, X. Li, H. P. Hratchian, A. F. Izmaylov, J. Bloino, G. Zheng, J. L. Sonnenberg, M. Hada, M. Ehara, K. Toyota, R. Fukuda, J. Hasegawa, M. Ishida, T. Nakajima, Y. Honda, O. Kitao, H. Nakai, T. Vreven, J. J. A. Montgomery, J. E. Peralta, F. Ogliaro, M. Bearpark, J. J. Heyd, E. Brothers, K. N. Kudin, V. N. Staroverov, R. Kobayashi, J. Normand, K. Raghavachari, A. Rendell, J. C. Burant, S. S. Iyengar, J. Tomasi, M. Cossi, N. Rega, J. M. Millam, M. Klene, J. E. Knox, J. B. Cross, V. Bakken, C. Adamo, J. Jaramillo, R. Gomperts, R. E. Stratmann, O. Yazyev, A. J. Austin, R. Cammi, C. Pomelli, J. W. Ochterski, R. L. Martin, K. Morokuma, V. G. Zakrzewski, G. A. Voth, P. Salvador, J. J. Dannenberg, S. Dapprich, A. D. Daniels, O. Farkas, J. B. Foresman, J. V. Ortiz, J. Cioslowski and D. J. Fox, in Gaussian 09 Rev. D.01, Wallingford CT, Gaussian Inc. 2013.